

## STELLAR EVOLUTION IN NGC 6791: MASS LOSS ON THE RED GIANT BRANCH AND THE FORMATION OF LOW MASS WHITE DWARFS<sup>1,2</sup>

JASONJOT S. KALIRAI<sup>3,4</sup>, P. BERGERON<sup>5</sup>, BRAD M. S. HANSEN<sup>6</sup>, DANIEL D. KELSON<sup>7</sup>,  
 DAVID B. REITZEL<sup>6</sup>, R. MICHAEL RICH<sup>8</sup>, AND HARVEY B. RICHER<sup>8</sup>

*Draft version November 4, 2018*

### ABSTRACT

We present the first detailed study of the properties (temperatures, gravities, and masses) of the NGC 6791 white dwarf population. This unique stellar system is both one of the oldest (8 Gyr) and most metal-rich ( $[Fe/H] \sim +0.4$ ) open clusters in our Galaxy, and has a color-magnitude diagram (CMD) that exhibits both a red giant clump and a much hotter extreme horizontal branch. Fitting the Balmer lines of the white dwarfs in the cluster, using Keck/LRIS spectra, suggests that most of these stars are undermassive,  $\langle M \rangle = 0.43 \pm 0.06 M_{\odot}$ , and therefore could not have formed from canonical stellar evolution involving the helium flash at the tip of the red giant branch. We show that at least 40% of NGC 6791's evolved stars must have lost enough mass on the red giant branch to avoid the flash, and therefore did not convert helium into carbon-oxygen in their core. Such increased mass loss in the evolution of the progenitors of these stars is consistent with the presence of the extreme horizontal branch in the CMD. This unique stellar evolutionary channel also naturally explains the recent finding of a very young age (2.4 Gyr) for NGC 6791 from white dwarf cooling theory; helium core white dwarfs in this cluster will cool  $\sim 3$  times slower than carbon-oxygen core stars and therefore the corrected white dwarf cooling age is in fact  $\gtrsim 7$  Gyr, consistent with the well measured main-sequence turnoff age. These results provide direct empirical evidence that mass loss is much more efficient in high metallicity environments and therefore may be critical in interpreting the ultraviolet upturn in elliptical galaxies.

*Subject headings:* open clusters and associations: individual (NGC 6791) - stars: evolution - stars: mass loss - techniques: photometric, spectroscopic - white dwarfs

### 1. INTRODUCTION

The advent of wide-field imaging cameras on 4-meter class telescopes in the last decade has led to a number of large homogeneous surveys of the Galactic open star cluster population. These studies not only shed light on cluster properties (e.g., distances, stellar content, ages, and metallicities) and their formation mechanisms, they also directly help in our understanding of the evolution and chemical structure of the Galactic disk. For example, the WIYN Open Cluster Survey (Mathieu 2000) and

<sup>1</sup> Data presented herein were obtained at the W. M. Keck Observatory, which is operated as a scientific partnership among the California Institute of Technology, the University of California, and the National Aeronautics and Space Administration. The Observatory was made possible by the generous financial support of the W. M. Keck Foundation.

<sup>2</sup> Based on observations obtained at the Canada-France-Hawaii Telescope (CFHT) which is operated by the National Research Council of Canada, the Institut National des Sciences de l'Univers of the Centre National de la Recherche Scientifique of France, and the University of Hawaii.

<sup>3</sup> University of California Observatories/Lick Observatory, University of California at Santa Cruz, Santa Cruz CA, 95060; jkalirai@ucolick.org

<sup>4</sup> Hubble Fellow

<sup>5</sup> Département de Physique, Université de Montréal, C.P. 6128, Succ. Centre-Ville, Montréal, Québec, Canada, H3C 3J7; bergeron@astro.umontreal.ca

<sup>6</sup> Department of Physics and Astronomy, Box 951547, Knudsen Hall, University of California at Los Angeles, Los Angeles CA, 90095; hansen/rmr/reitzel@astro.ucla.edu

<sup>7</sup> Carnegie Observatories, Carnegie Institution of Washington, 813 Santa Barbara Street, Pasadena CA, 91101; kelson@ociw.edu

<sup>8</sup> Department of Physics and Astronomy, University of British Columbia, Vancouver, British Columbia, Canada, V6T 1Z1; richer@astro.ubc.ca

the CFHT Open Cluster Survey (Kalirai et al. 2001a) have now targeted several dozens of these systems in our Galaxy (e.g., NGC 6819 – Kalirai et al. 2001b; NGC 2099 – Kalirai et al. 2001c; NGC 2168 and NGC 2323 – von Hippel et al. 2002 and Kalirai et al. 2003).

NGC 6791 is a relatively nearby star cluster ( $d \sim 4$  kpc – Chaboyer, Green, & Liebert 1999) located at  $(l, b) = (69.96^{\circ}, 10.90^{\circ})$ . Very early studies of the system established it as one of the most populous open star clusters, with a mass of several thousand Solar masses (e.g., Kinman 1965). These first studies also concluded that NGC 6791's stellar content is both very old and has a high metal abundance (e.g., Spinrad & Taylor 1971). More recent studies have confirmed these earlier results with greater precision; current best estimates indicate that the age of NGC 6791 is  $\gtrsim 8$  Gyr, the  $[\alpha/Fe]$  is Solar (Origlia et al. 2006), and the metallicity is  $[Fe/H] = +0.3 - +0.5$  (Kaluzny 1990; Demarque, Green, & Guenther 1992; Montgomery, Janes, & Phelps 1994; Peterson & Green 1998; Chaboyer, Green, & Liebert 1999; Stetson, Bruntt, & Grundahl 2003; Carney, Lee, & Dodson 2005; Gratton et al. 2006; Origlia et al. 2006). The cluster therefore ranks as both one of the oldest open clusters and one of the most metal-rich in our Galaxy (Friel & Janes 1993). Given this unique combination, NGC 6791 currently serves as the high metallicity anchor when measuring star formation histories from CMDs of nearby galaxies.

The CMD of NGC 6791 exhibits some peculiar features (e.g., Stetson et al. 2003). The cluster contains a large blue straggler population, and both a red giant clump and an extremely blue horizontal branch. Given the high

metallicity, this is a strong example of the second parameter effect. The extreme horizontal branch has very likely formed as a result of increased mass loss in post main-sequence evolutionary phases, possibly due to the high metallicity of the cluster (Faulkner 1972; Sweigart 1987; Castellani & Castellani 1993). Although the presence of these stars in the field has been suggested to possibly arise from binary evolution (e.g., Allard et al. 1994; Maxted et al. 2001; Han et al. 2003), this does not appear to be the case in star clusters (e.g., Moni Bidin et al. 2006a), especially a system like NGC 6791 (see discussion in § 7.1). The cluster orbit is highly eccentric, which combined with its chemical content and position, has led to suggestions that it may even represent the nucleus of a tidally disrupted galaxy (Carraro et al. 2006). The unique properties of NGC 6791 certainly hold promising information on its origins and past dynamical and stellar evolutionary history.

Recently, King et al. (2005) produced the deepest CMD for NGC 6791 to date. Using the Hubble Space Telescope (*HST*) Advanced Camera for Surveys, they observed the cluster for 4 orbits, reaching a limiting magnitude of  $F606W = 28$ . The resulting CMD shows a tightly constrained main-sequence to the limit of the data and, for the first time, has uncovered a large population of hundreds of white dwarfs in the cluster (Bedin et al. 2005). These stellar remnants are cooling with age, becoming fainter as time passes, and therefore serve as *clocks* from which the cluster can be dated (see e.g., Hansen et al. 2004 for a detailed discussion). This technique of determining ages of star clusters from white dwarf cooling theory successfully reproduces independently measured main-sequence turnoff ages in the six other open clusters, and two globular clusters, that have been tested to date (von Hippel 2005; Hansen et al. 2004, 2007). However, Bedin et al. (2005) conclude that the white dwarf cooling age of NGC 6791 is in fact 2.4 Gyr, a factor of three less than the well measured main-sequence turnoff age. Such a discrepancy clearly adds to the list of peculiarities of this cluster.

In this paper we present evidence that the white dwarf population of NGC 6791 is unlike that in other clusters. The formation of most of these stars has resulted from a unique evolutionary channel involving significant mass loss on the red giant branch, leading to a final mass below the critical mass needed to ignite helium in the core of the star (Hansen 2005). Hence, the progenitors of these white dwarfs avoided the helium flash and therefore the cores of the white dwarfs are composed of helium and not carbon-oxygen. As a result, the masses of the white dwarfs are well below the expected  $0.5 - 0.6 M_{\odot}$  value that the canonical channel produces for these initial masses. Invoking helium core white dwarf models (Hansen 2005) in the fit of the white dwarf cooling sequence from Bedin et al. (2005) yields a consistent age for the cluster as measured from the turnoff.

In the next section, we discuss our imaging data set for NGC 6791. We present a new CMD of the cluster in § 3, discuss its various features, and estimate an age for the cluster from the new data. Next, we summarize the findings of Bedin et al. (2005) and consider possible explanations in § 4. The first spectroscopic observations of NGC 6791's white dwarf population are presented in § 5 and § 6 and temperatures, gravities, and masses for these

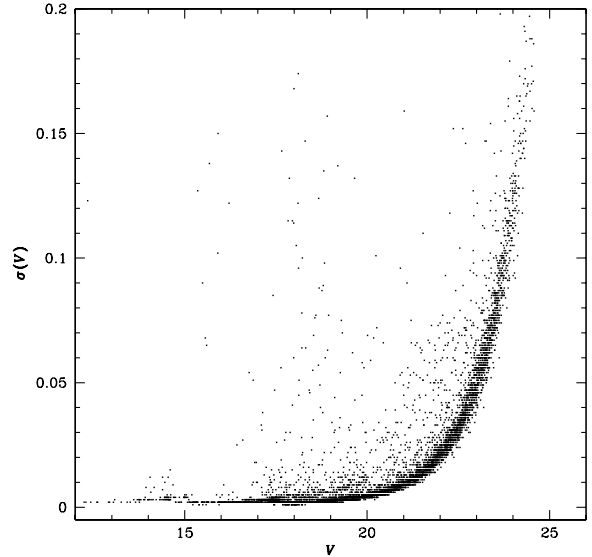


FIG. 1.— The DAOPHOT photometric error, as a function of  $V$  magnitude indicates the photometry is accurate to  $V \gtrsim 24$  (where the error is  $\sigma_V = 0.12$  magnitudes).

stars are derived in § 6.1. The results and their implications are discussed in § 7 and the study is summarized in § 8.

## 2. IMAGING OBSERVATIONS

We imaged NGC 6791 with the CFH12K mosaic CCD on the Canada-France-Hawaii Telescope (CFHT) in March and April of 2001. This camera contains 12 CCDs, each with  $2048 \times 4096$  pixels, where each pixel subtends  $0''.206$ . The detector projects to an area of  $42' \times 28'$  on the sky, much larger than the size of the cluster. The observations were taken in the  $B$  and  $V$  bands with the center of the cluster placed on one of the CCDs (away from the center of the mosaic where stars would be lost due to chip gaps). Seven exposures were taken in each filter (each one 850 seconds in  $V$  and 1150 seconds in  $B$ ) to achieve a photometric depth fainter than  $B, V \sim 24$  over a magnitude fainter than the brightest expected cluster white dwarfs. Shallower exposures were also obtained to obtain photometry of the brighter stars that were saturated on the deeper exposures. Most observations were obtained in sub-arcsecond seeing and all were taken under photometric skies. Table 1 presents a complete observational log of the imaging data.

The data were processed (flat-field, bias and dark corrected) and montaged using the FITS Large Images Processing Software<sup>9</sup> (FLIPS) as described in Kalirai et al. (2001a). The photometry of all sources was performed using a variable point-spread function in DAOPHOT (Stetson 1994). The photometry was calibrated using Landolt standard star fields as discussed in §§ 5.1 and 5.2 of Kalirai et al. (2001a). The mean errors in the photometry are  $\sigma_V = 0.02$  mag at  $V = 22$ ,  $\sigma_V = 0.05$  mag at  $V = 23$ , and  $\sigma_V = 0.12$  mag at  $V = 24$ . A statistical error plot for several thousand stars in the vicinity of the cluster is shown in Figure 1.

Figure 2 shows a starcount map constructed from our CFHT imaging observations. We have included all ob-

<sup>9</sup> <http://www.cfht.hawaii.edu/~jcc/Flips/flips.html>

TABLE 1

Filter	Exp. Time (s)	No. Images	Seeing (")	Airmass
<i>V</i>	850	7	0.63 – 0.98	<1.25
<i>V</i>	300	1	0.93	1.25
<i>V</i>	90	1	1.03	1.26
<i>V</i>	20	1	0.86	1.09
<i>V</i>	10	1	0.92	1.26
<i>V</i>	5	1	1.03	1.28
<i>V</i>	1	1	1.02	1.28
<i>B</i>	1150	7	0.87 – 1.30	<1.21
<i>B</i>	400	1	0.86	1.14
<i>B</i>	120	1	0.98	1.15
<i>B</i>	30	1	1.07	1.09
<i>B</i>	10	1	0.75	1.12
<i>B</i>	5	1	0.73	1.12
<i>B</i>	1	1	0.79	1.12

jects within a generous envelope of the cluster main sequence on the CMD (see § 3). With this mild cut, NGC 6791 stands out very strongly against the foreground/background Galactic disk stars. The rectangular region marks the Keck LRIS field of view over which we obtained spectroscopy of white dwarf candidates (see § 5).

### 3. THE COLOR-MAGNITUDE DIAGRAM OF NGC 6791

The CMD for NGC 6791 is presented in Figure 3 for all stars that fall within an area slightly larger than the Keck LRIS spectroscopic mask shown in Figure 2. The CMD clearly shows all of the major phases of stellar evolution: the main-sequence, turnoff, subgiant branch, red giant branch, and red giant clump. A significant population of potential blue straggler stars is also seen above the cluster turnoff.

The red giant clump of NGC 6791 represents a phase of core helium burning following the helium flash at the tip of the cluster's red giant branch. The result of this burning is a star with a carbon-oxygen core. As has been noted in earlier studies (e.g., Kaluzny & Udalski 1992; Liebert, Saffer, & Green 1994; Kaluzny & Rucinski 1995; Green, Liebert, & Peterson 1996), the NGC 6791 CMD also shows about a dozen extreme horizontal branch stars (at  $B-V \sim 0$ ,  $V \sim 17$ ), most of which are likely subdwarf B and subdwarf O stars. Although these much hotter stars are also burning helium in their cores, their evolution has differed from the red giant clump stars. These stars likely represent the products of increased mass loss on the red giant branch (Faulkner 1972) and possibly suffered a delay in the ignition of the core helium in the star until a point where the star contracted further (Lanz et al. 2004; Castellani & Castellani 1993). In this picture of single star evolution, it is believed that the high metallicity of the cluster is driving the enhanced mass loss (e.g., D'Cruz et al. 1996). Yong, Demarque, & Yi (2000) also consider whether mass loss on the horizontal branch itself could have led, in part, to the morphology of the extreme horizontal branch of this cluster.

In the faint-blue part of the CMD in Figure 3 we see a population of white dwarf candidates. Given the richness of NGC 6791 and the position of our spectroscopic mask (see Figure 2), we statistically expect most of the white dwarfs in our sample to be a part of the cluster. The starcount map in Figure 2 shows that NGC 6791 is centered in the top row CCDs, slightly to the right of the

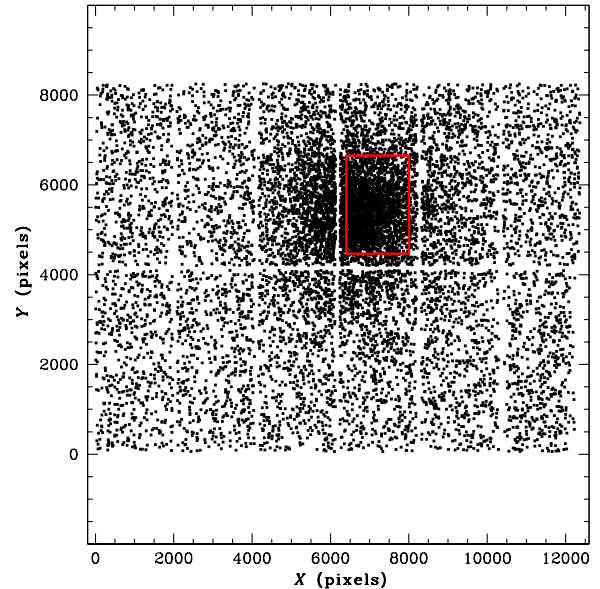


FIG. 2.— A wide-field starcount map of NGC 6791 constructed from the CFHT imaging. A mild cut has been used to isolate stars within an envelope of the cluster main sequence. The region in which spectroscopic targets were selected for Keck/LRIS observations is indicated with a rectangle (see § 5).

center of the camera. We can directly measure the field white dwarf density by examining the faint-blue end of a CMD constructed from the outer CCDs in the bottom row. We take a region with an area  $\gtrsim 4 \times$  our LRIS field and count a dozen stellar objects within the same magnitude and color range that we use for selecting white dwarf targets (see § 5). Scaling by the ratio of areas, the number of field white dwarfs in our sample is therefore expected to be  $\lesssim 3$ .

### 3.1. Cluster Reddening, Distance, Age, and Metallicity

The foreground reddening, distance, age, and metallicity of NGC 6791 have been estimated many times in the literature (see references in § 1). Recent values based on *HST* filters (King et al. 2005), *B, V, I* optical data (Chaboyer, Green, & Liebert 1999; Stetson, Bruntt, & Grundahl 2003), and *J, H, K* near infrared observations (Carney, Lee, & Dodson 2005) find  $E(B-V) = 0.09 - 0.18$ . The same studies estimate the distance of NGC 6791 to be  $d \sim 4000$  pc (the range in these studies is  $d = 3600 - 4200$  pc). Most determinations of the age of NGC 6791 have resulted from fitting theoretical isochrones to the observed cluster main sequence and turnoff morphology. Such determinations are strongly dependent on the assumed reddening, distance, and metallicity. Differences in the input physics within various groups theoretical models (e.g., helium abundance and treatment of overshooting) also play an appreciable role in the age determinations. Therefore, recent values in the literature have ranged from  $\sim 8$  Gyr (e.g., Chaboyer, Green, & Liebert 1999) to as high as 12 Gyr (e.g., Stetson, Bruntt, & Grundahl 2003). As we mentioned earlier, the cluster has been known to have a high metal abundance for some time. The first medium resolution spectroscopy found  $[Fe/H] = +0.40 \pm 0.10$  (Peterson & Green 1998). Two very recent studies based on high resolution infrared spectroscopy (Origlia et al. 2006) and high resolution optical spectroscopy (Gratton

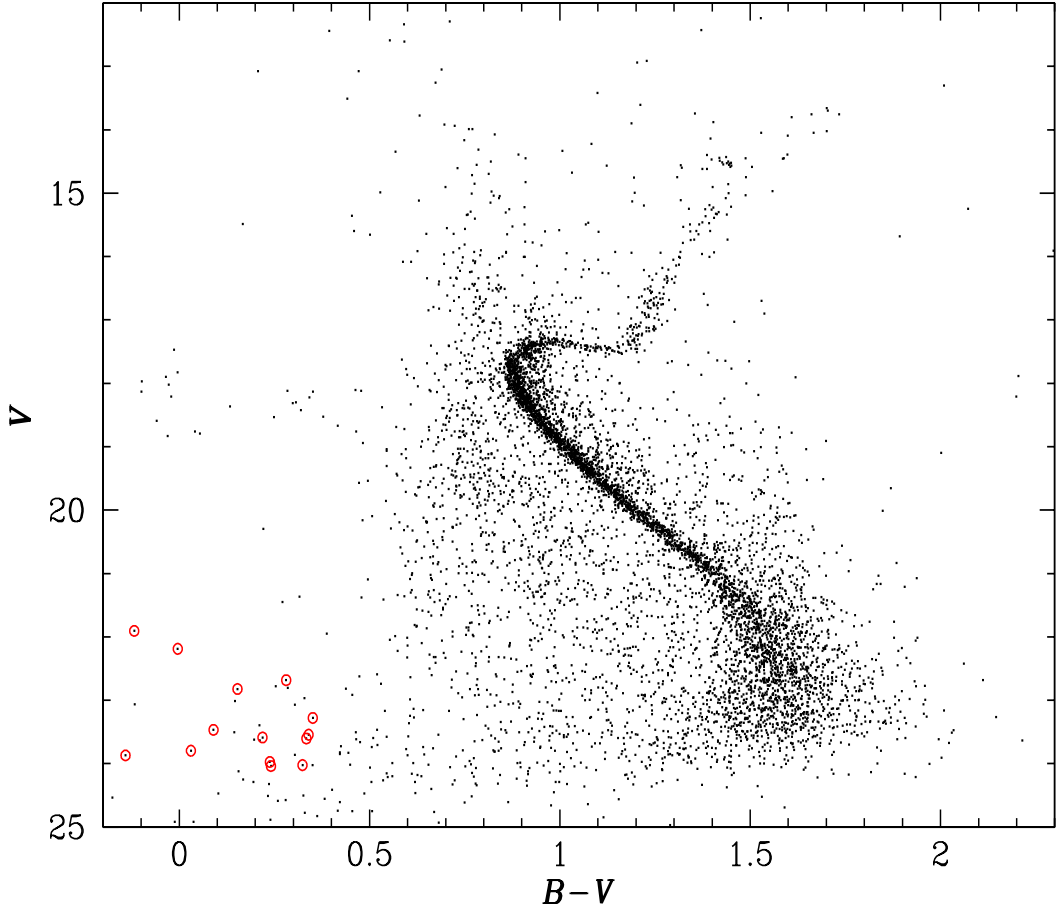


FIG. 3.— The CMD of NGC 6791 from our CFHT CFH12K imaging data. A very tight cluster main-sequence, and several post main-sequence evolutionary phases can be clearly seen. Roughly a dozen bright, extremely blue horizontal branch stars are also evident at  $B-V \sim 0$ ,  $V \sim 17$ . The faint, blue region of the CMD shows several potential white dwarf candidates. The 14 objects that were targeted with Keck/LRIS are highlighted with larger open circles (see § 5).

et al. 2006) confirm this. Origlia et al. (2006) find  $[\text{Fe}/\text{H}] = +0.35 \pm 0.02$  and Gratton et al. (2006) find  $[\text{Fe}/\text{H}] = +0.47 \pm 0.04$ .

Our CMD of NGC 6791 can be used to independently determine the age of the cluster. We find that for a choice of  $E(B-V) = 0.14$  (Carney, Lee, & Dodson 2005),  $(m - M)_0 = 13.0$  (an average of the four recent studies referenced above), and  $[\text{Fe}/\text{H}] = +0.37$ , an isochrone with  $[\alpha/\text{Fe}] = 0$  and age = 8.5 Gyr (VandenBerg, Bergbusch, & Dowler 2005) provides an excellent fit to the observed CMD. This is shown in Figure 4. Adopting a slightly larger metallicity (e.g.,  $[\text{Fe}/\text{H}] = +0.47$  – Gratton et al. 2006) requires a younger age by  $\sim 1$  Gyr. However the fit is significantly worse along the subgiant and red giant branches. Similar variations in the reddening and distance modulus also produce smaller age changes. Therefore, our data supports the literature results that the cluster is very old, and metal-rich. In a future paper, we will provide a full analysis of the entire data set in the CFHT mosaic image. This will include the first determination of the cluster’s distance, age, reddening, binary fraction, and mass based on MonteCarlo simulations of synthetic CMDs. These comparisons, as shown in Kalirai & Tosi (2004) for several open clusters, allow

modeling of several additional parameters which dictate the distribution of points in the CMD, such as stochastic star formation processes, photometric spread, data incompleteness, and cluster luminosity function.

#### 4. A WHITE DWARF COOLING AGE FOR NGC 6791 OF 2.4 GYR?

Up until recently, all of the studies that have measured the age of the cluster used the same technique, isochrone fitting of the main-sequence turnoff. Recently, Bedin et al. (2005) have imaged NGC 6791 with the *HST* Advanced Camera for Surveys down to very faint magnitudes (F606W = 28). Their study was the first to uncover the remnant population of evolved stars in the cluster (see their Figure 1). Since these stars have no remaining nuclear energy sources, they cool with time and become predictably fainter. Bedin et al. (2005) model the observed luminosity function of these white dwarfs and provide the first independent age measurement for the cluster. Given the morphology and peak of the observed white dwarf luminosity function, white dwarf cooling models from Salaris et al. (2000) indicate that the cluster is only 2.4 Gyr old. This age is at least a factor of three less than the main-sequence turnoff age for the cluster.

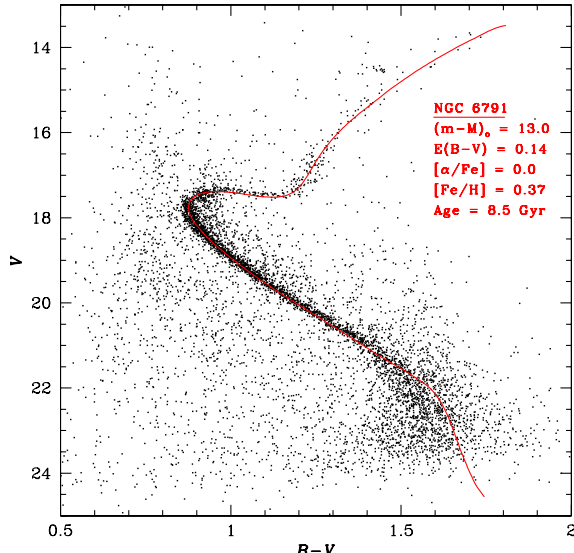


FIG. 4.— An 8.5 Gyr isochrone with  $[Fe/H] = +0.37$  (VandenBerg, Bergbusch, & Dowler 2005) provides an excellent fit to the main-sequence, turnoff, sub-giant branch, and red giant branch of NGC 6791. These data therefore support previous findings that the cluster is both very old and metal rich.

#### 4.1. Possible Explanations

Bedin et al. (2005) consider several explanations for the white dwarf (WD) cooling age discrepancy in NGC 6791 but find that none of them are very satisfactory. These include using radically different initial-to-final mass mappings, incorrect distance moduli or metallicities, different hydrogen-layer thicknesses for the WDs, and binary evolution.

At least two additional theories have been proposed to explain the above anomalous age result that are more promising. The first suggests that the cooling rate of white dwarfs may be retarded in a system such as NGC 6791 given the high metallicity of the cluster. DeJoye & Bildsten (2002) predicted that gravitational settling of  $^{22}\text{Ne}$  would result in an increased release of gravitational energy that may not be seen in other less metal-rich systems. In fact, they explicitly say that a cluster such as NGC 6791 is an ideal environment to test this effect. However, the magnitude of the delay is predicted to be 0.25 – 1.6 Gyr (although it does depend on an uncertain diffusion coefficient) so it is not clear whether it, or it alone, can explain the observed discrepancy in the turnoff and white dwarf cooling ages of NGC 6791. L. Bildsten (2007, private communication) is in the process of investigating this possible explanation further.

The second scenario proposed by Hansen (2005), suggests that mass-loss on the red giant branch may be the culprit. Given the higher metallicity in NGC 6791, theoretical models of stellar evolution (e.g., Marigo 2001) predict that post-main sequence stars in this cluster would lose more mass than in less metal-rich systems (see § 7.3). If some stars can expel enough mass on the red giant branch, they may be peeling away towards the white dwarf cooling phase before reaching the helium flash. Therefore, the use of carbon-oxygen core white dwarf models to date NGC 6791 will yield an incorrect age measurement. It is interesting to note that a fit to he-

lium core white dwarf models recovers an age that is roughly  $3\times$  larger than the Bedin et al. (2005) result, and therefore consistent with the main-sequence turnoff age (Hansen 2005). In the next section, we test this hypothesis.

Although not as extreme a case, it is worth noting that we have seen hints for the dependence of mass loss on metallicity in another set of clusters. Both the Hyades (Perryman et al. 1998) and NGC 2099 (Kalirai et al. 2001c; 2005a) are of similar age, yet their metallicities differ by a factor of two ( $[Fe/H]_{\text{Hyades}} = +0.17$  and  $[Fe/H]_{\text{NGC 2099}} = -0.1$ ). An initial-to-final mass relationship based on spectroscopically observed white dwarfs in these two clusters (Claver et al. 2001; Kalirai et al. 2005a) suggests that stars in NGC 2099, through their evolution, have lost less mass than stars in the Hyades. The mean mass of white dwarfs in NGC 2099 is  $M = 0.80 \pm 0.03 M_{\odot}$  whereas white dwarfs in the Hyades have  $M = 0.72 \pm 0.02 M_{\odot}$ .

#### 4.1.1. Mass Loss on the Red Giant Branch: Testing the Theory

The presence of two distinct phases of core-helium burning in this cluster (the red giant clump and the extreme horizontal branch) hints that mass loss is stochastic in this cluster. For a metallicity of  $[Fe/H] = +0.4$ , the critical mass needed to ignite helium in the core of a star is  $0.45 - 0.47 M_{\odot}$  (Dominguez et al. 1999; Pietrinferni et al. 2004; VandenBerg, Bergbusch, & Dowler 2005; L. Girardi 2006, private communication). Therefore, a direct prediction of Hansen (2005) is that a large fraction of the white dwarfs along the Bedin et al. (2005) cooling sequence should have masses less than this critical mass. Such objects are very rare, both in other star clusters and in the field (e.g., from the Palomar Green Survey – see Liebert, Bergeron, & Holberg 2005), and therefore their discovery would almost certainly validate this suggestion.

#### 5. SPECTROSCOPIC OBSERVATIONS

We obtained multi-object spectroscopic observations of the brightest white dwarf candidates detected in our CFHT imaging study with the Keck I telescope on 3–4 August 2005. We designed a single mask and targeted 14 objects with the Low Resolution Imaging Spectrometer (LRIS – Oke et al. 1995) over the  $5' \times 7'$  field of view. These objects were selected based on their magnitudes, colors, and location within our much larger CFHT field of view. The spectra were obtained using the 600/4000 grism which simultaneously covers 2580 Å. The total exposure time was 21,600 seconds. The seeing was variable during the run, ranging from  $0''.5$  to  $1''.1$ .

The spectra were reduced using python routines specifically written for LRIS data and are described in detail in Kelson et al. (2000) and Kelson (2003). To summarize the key steps, the individual exposures were first bias subtracted using the overscan region. Next, the vertical distortion (spatial axis) was measured using cross-correlations along the slit edges of the spectroscopic flat-fields, and the boundaries of the slitlets were identified using Laplacian edge-detection. The wavelength calibration was performed in an automated way using the Hg, Cd, Zn, Ne lamp lines and the zero-points of the dispersion solutions were refined using night sky emission lines. The *rms* scatter about the dispersion solutions was

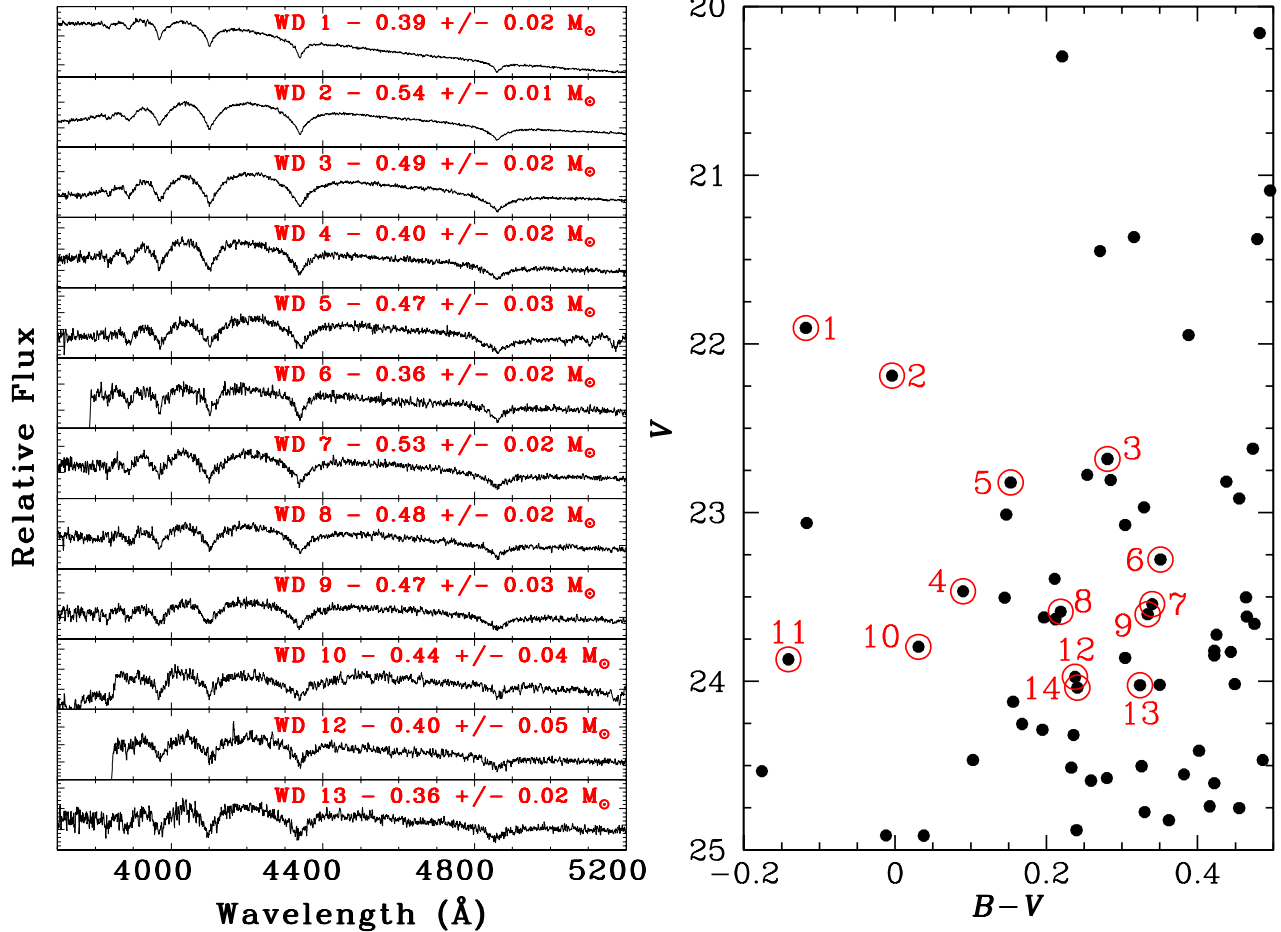


FIG. 5.— *Left* - Keck/LRIS spectra confirm that 12 of the 14 faint-blue targets in our spectroscopic sample are in fact white dwarfs. The spectra of these stars show broad hydrogen Balmer lines that we fit to model line profiles to derive individual stellar masses (indicated within each panel – see § 6.1). The spectra for two of the faintest targets were of poor quality and did not permit an accurate classification of the objects. *Right* - The white dwarf region of the CMD is shown with identifications marking each of the spectroscopically targeted stars (larger open circles). The identifications are consistent with those in the adjacent panel displaying the spectra for these stars.

typically  $<0.05$  pixels. The data were corrected for pixel-to-pixel variations by dividing by a normalized spectral flat-field. The spectrum of the night sky was fitted for, and subtracted off, using bivariate cubic B-splines fit to the data on both sides of the targets. Finally, one-dimensional spectra were extracted and coadded using standard IRAF task and flux calibrated using a spectrophotometric standard star (HZ 21).

## 6. THE SPECTRA OF WHITE DWARFS IN NGC 6791

In Figure 5 (left) we present the optical spectra for 12 of the 14 faint-blue objects that were targeted with LRIS on Keck I. As discussed earlier, most of these objects are likely to be cluster members and therefore must be white dwarfs. The spectra confirm this. All of these objects show pressure broadened Balmer lines, from  $H\beta$  at  $4861\text{ \AA}$  to higher order lines up to  $H9$  at  $3835\text{ \AA}$ , a clear signature of DA white dwarfs. The two objects not shown (WDs 11 and 14) were among the faintest objects targeted and the spectra do not contain enough signal-to-noise to classify the objects. The right panel shows the faint-blue region of the cluster CMD with the 12 objects indicated as large open circles. The two objects for which the spectra are not shown are also indicated.

Although the Balmer lines are the most prominent fea-

tures in these white dwarf spectra, a closer look reveals other interesting features in two stars. Towards the red end of our spectral coverage for WD 5, we see evidence for additional absorption lines. Similarly, the spectrum of WD 10 shows some contaminating lines. These objects therefore may represent DA+dM binary systems. Fortunately, LRIS is a dual beam spectrograph and therefore we have simultaneous observations of these stars extending to beyond  $7500\text{ \AA}$ . A reduction of those data for these targets should reveal any counterparts and certainly lead to a better understanding of the nature of these objects.

### 6.1. Determining $T_{\text{eff}}$ , $\log g$ , and Masses for NGC 6791's White Dwarf Population

We determine the effective temperatures ( $T_{\text{eff}}$ ) and gravities ( $\log g$ ) for the twelve white dwarfs shown in Figure 5 using the techniques described in Bergeron, Saffer, & Liebert (1992). These parameters are calculated for each white dwarf using the nonlinear least-squares method of Levenberg-Marquardt (Press, Flannery, & Teukolsky 1986). For combinations of these values,  $\chi^2$  is minimized using normalized model line profiles of *all* absorption lines simultaneously. These fits are shown in Figure 6. For WD 1 – WD 9, the spectra have very well

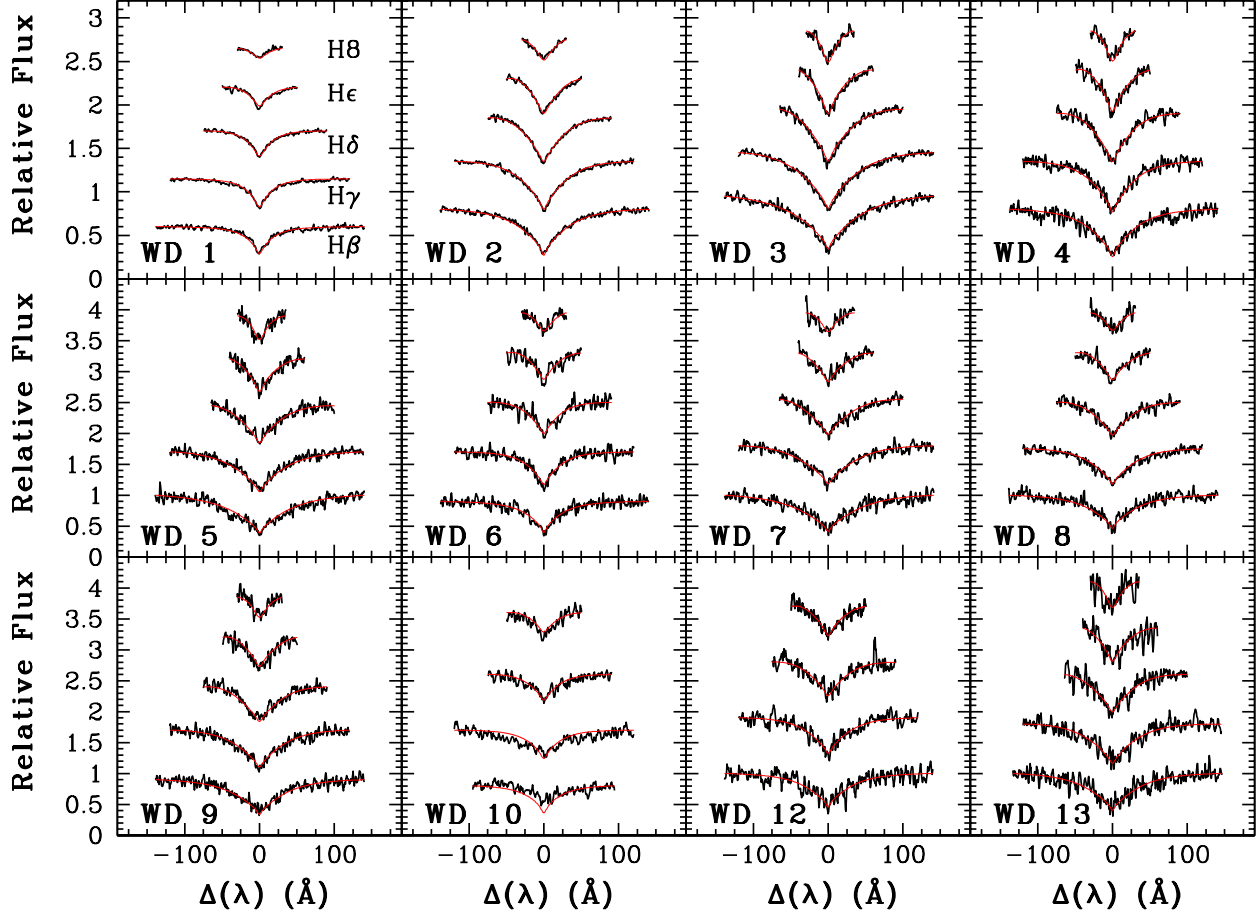


FIG. 6.— Individual hydrogen Balmer lines are shown for 12 white dwarfs in NGC 6791 (see Figure 5 for identifications). Within each panel, the lines for a given white dwarf are H $\beta$  (bottom), H $\gamma$ , H $\delta$ , He, and H8 (top). Spectroscopic fits, simultaneously to all lines, constrain the  $T_{\text{eff}}$ ,  $\log g$ , and mass of each white dwarf as discussed in § 6.1 (smooth profiles). For WD 1 – WD 4, the H9 Balmer line at 3835 Å was also used in the fits (not shown). The uncertainties on  $T_{\text{eff}}$  and  $\log g$  for WD 10, WD 12, and WD 13 are larger than for the other white dwarfs as discussed in the text. Table 2 summarizes the results from these fits.

characterized higher order Balmer lines (e.g., at least H8 and up to H9 for four stars – WD 1, WD 2, WD 3, and WD 4) and the model atmosphere fits to all lines are excellent. For WD 10 and WD 12, the spectra are truncated shortward of  $\sim 3850$  Å as a result of the locations of these stars on the spectroscopic mask (close to one of the edges). Nevertheless, He is cleanly measured in both stars and so we measure  $T_{\text{eff}}$  and  $\log g$ , although these parameters will have larger errors. For WD 10, the best fit model does not agree with the shape of the H $\beta$  line which may be contaminated. We discuss this object further below. Finally, WD 13 shows five Balmer lines (H $\beta$  – H8) even though this star is our faintest white dwarf and therefore the spectrum is somewhat noisier. Again, the measurements for this star will have larger uncertainties than the other higher signal-to-noise data.

The derivation of masses of white dwarfs from modeling the hydrogen Balmer lines has been shown to yield consistent results when compared to independent mass measurements, such as from gravitational redshifts (Bergeron, Liebert, & Fulbright 1995). We determine the mass for each white dwarf by interpolating the  $T_{\text{eff}}$  and  $\log g$  within the updated evolutionary models of Fontaine, Brassard, & Bergeron (2001). Our standard model has a surface hydrogen layer mass fraction of  $q(\text{H})$

$= M_{\text{H}}/M = 10^{-4}$  and helium layer of  $q(\text{He}) = 10^{-2}$ . For the uncertainties in the masses, we note that if these white dwarfs are the products of strong mass loss on the red giant branch, they may be less massive than typical field white dwarfs. Surface gravities of less massive white dwarfs can be sensitive to the adopted hydrogen layer thickness, and so we have calculated a new suite of low-mass, helium core white dwarf models, using the models of Hansen & Phinney (1998), and considering a full range of  $q(\text{H})$  up to very thick layers,  $q(\text{H}) = 10^{-2}$ . Therefore, we determine the range of acceptable masses by considering this full range of  $q(\text{H})$  in addition to the errors on  $T_{\text{eff}}$  and  $\log g$ .

We find that the mean mass of the twelve white dwarfs in our sample is  $0.44 M_{\odot}$ . Three of the stars have masses below  $0.40 M_{\odot}$ , five of the stars have masses of  $0.40$  –  $0.47 M_{\odot}$ , and only four objects have masses greater than  $0.47 M_{\odot}$ . The uncertainties on the individual mass measurements are typically  $0.02 M_{\odot}$  and at worst  $0.05 M_{\odot}$  for one star. These results clearly suggest that the white dwarf population of NGC 6791 is indeed notably undermassive when compared to both other star clusters and the field distribution (see below). As we discussed earlier, this is likely linked to the evolution of the progenitors of these white dwarfs.

TABLE 2

ID	$\alpha_{J2000}$	$\delta_{J2000}$	$V$	$\sigma_V$	$B - V$	$\sigma_{B-V}$	$T_{\text{eff}}$ (K)	$\log g$	$M (M_{\odot})$	$t_{\text{cool}}^a$ (Gyr)
WD 1	19:20:48.6	37:45:48.4	21.91	0.03	-0.12	0.04	$34,700 \pm 100$	$7.30 \pm 0.03$	$0.39 \pm 0.02$	$<0.14$
WD 2 <sup>b</sup>	19:21:04.1	37:44:43.3	22.19	0.03	0.00	0.04	$19,400 \pm 100$	$7.88 \pm 0.02$	$0.54 \pm 0.01$	$0.063 \pm 0.001$
WD 3 <sup>b</sup>	19:21:10.5	37:45:51.2	22.68	0.04	0.28	0.06	$13,000 \pm 400$	$7.80 \pm 0.04$	$0.49 \pm 0.02$	$1.01 \pm 0.82 (0.25 \pm 0.02)$
WD 4	19:20:58.4	37:45:55.5	23.47	0.08	0.09	0.11	$17,100 \pm 200$	$7.50 \pm 0.04$	$0.40 \pm 0.02$	$0.48 \pm 0.39$
WD 5 <sup>b</sup>	19:20:47.3	37:44:37.3	22.82	0.03	0.15	0.05	$12,500 \pm 300$	$7.76 \pm 0.08$	$0.47 \pm 0.03$	$1.23 \pm 1.01 (0.26 \pm 0.03)$
WD 6	19:20:48.2	37:47:18.1	23.28	0.06	0.35	0.10	$21,500 \pm 500$	$7.33 \pm 0.07$	$0.36 \pm 0.02$	$<0.53$
WD 7	19:20:42.5	37:44:12.9	23.54	0.07	0.34	0.12	$14,800 \pm 300$	$7.91 \pm 0.06$	$0.53 \pm 0.02$	$0.15 \pm 0.02$
WD 8	19:21:13.6	37:43:20.0	23.59	0.08	0.22	0.12	$18,200 \pm 300$	$7.73 \pm 0.06$	$0.48 \pm 0.02$	$0.40 \pm 0.31 (0.07 \pm 0.01)$
WD 9	19:20:56.9	37:44:15.2	23.60	0.09	0.33	0.14	$16,100 \pm 300$	$7.71 \pm 0.06$	$0.47 \pm 0.03$	$0.57 \pm 0.38 (0.11 \pm 0.01)$
WD 10	19:20:47.0	37:46:29.0	23.80	0.09	0.03	0.14	$27,700 \pm 600$	$7.52 \pm 0.11$	$0.44 \pm 0.04$	$<0.23$
WD 11	19:21:05.8	37:46:51.5	23.87	0.16	-0.14	0.20	—	—	—	—
WD 12	19:21:02.9	37:47:27.0	23.97	0.11	0.24	0.15	$17,600 \pm 600$	$7.50 \pm 0.13$	$0.40 \pm 0.05$	$0.48 \pm 0.44$
WD 13	19:21:08.3	37:44:30.2	24.02	0.12	0.32	0.19	$14,000 \pm 500$	$7.40 \pm 0.10$	$0.36 \pm 0.02$	$1.09 \pm 0.94$
WD 14	19:21:06.5	37:44:10.5	24.04	0.12	0.24	0.18	—	—	—	—

<sup>a</sup> Cooling ages calculated using helium core models, except for WD 2 and WD 7. Ages with carbon-oxygen core models for stars with  $M \geq 0.47 M_{\odot}$  in brackets.

<sup>b</sup> Possible non-cluster white dwarfs.

We summarize the derived parameters for each white dwarf in Table 2. We noted above that the best fit model for WD 10 did not reproduce the  $H\beta$  line well. As the mass for that star is  $0.44 M_{\odot}$ , ignoring it from the sample would not change the results. Also included in Table 2 is the cooling age of each star (last column). The default values are those derived using the models described above for helium cores, except for WD 2 and WD 7. These two stars both have  $M > 0.50 M_{\odot}$  and therefore we have used the standard 50/50 carbon-oxygen core models from Fontaine, Brassard, & Bergeron (2001) to derive ages. For four other white dwarfs with  $M \lesssim 0.50 M_{\odot}$ , in addition to the ages derived from helium core models we have also indicated the ages assuming the carbon-oxygen models in brackets. The uncertainties on the cooling ages, especially for the low mass stars, are large as we have considered a full range in the mass of the H layer as discussed above.

## 6.2. Confirming Cluster Membership

We noted earlier in § 3 that a blank field of equal area taken from the outer CCDs shows a very low density of faint-blue stellar objects. The expected contamination from such field white dwarfs in our CMD is approximately three objects. This is  $\sim 20\%$  of the number of stars targeted in our spectroscopic observations. The masses of the white dwarfs derived above support this. They are much lower than typical field white dwarfs and therefore these stars must belong to the cluster. For example, the mass distribution of the white dwarf sample in the Palomar Green (PG) Survey (Liebert, Bergeron, & Holberg 2005) peaks at a mass near  $0.6 M_{\odot}$ . For comparison to our NGC 6791 cluster white dwarfs, this sample of nearly 350 white dwarfs contains less than 25% stars with  $M < 0.54 M_{\odot}$ , 10% with  $M < 0.47 M_{\odot}$ , and 2.6% with  $M < 0.40 M_{\odot}$ . An independent estimate can be drawn from the much larger Sloan Digital Sky Survey, which now contains over 7000 white dwarfs in total (Kepler et al. 2007). For those 2896 stars with  $g' < 19$  (the spectral quality of white dwarfs in this sample is poorer than in the PG sample), the Sloan dataset contains 16% stars with  $M < 0.54 M_{\odot}$ , 6.3% with  $M < 0.47 M_{\odot}$ , and

3.3% with  $M < 0.40 M_{\odot}$ .

We can attempt to quantify which of our white dwarfs are field stars, if any. For this, we first calculate a theoretical color for each white dwarf using the Fontaine, Brassard, & Bergeron (2001) models and our measured values of  $T_{\text{eff}}$  and  $\log g$ . Comparing this color directly to our  $B - V$  photometry yields an estimate for the reddening of each star. This reddening, coupled with an estimate of the star's absolute magnitude (similarly calculated from the models), yields the estimated distance modulus for each star. For almost every white dwarf, the error in this distance modulus is dominated by the uncertainty in the extinction given the typical  $\gtrsim 0.1$  color error. Cluster membership can now be established by comparing these distance moduli and reddenings, for each star, to estimates for NGC 6791.

We find that nine of our twelve white dwarfs are consistent within the  $2\sigma$  range of cluster parameters. This suggests a 25% contamination fraction, slightly larger than our estimate based on the blank field earlier in § 3. Furthermore, all three objects that do not agree with the range of NGC 6791's distance moduli and reddening are at the high mass end of our sample, WD 2 ( $0.54 M_{\odot}$ ), WD 3 ( $0.49 M_{\odot}$ ), and WD 5 ( $0.47 M_{\odot}$ ). This latter object was also shown earlier to perhaps be in a binary system. Therefore, the mean mass of our sample of white dwarfs decreases to  $0.43 M_{\odot}$  if we exclude these three possible field white dwarfs. However, we note that two of the three excluded stars have a mass significantly less than the field distribution and therefore it is not definitive that they are non-members. The method used to estimate membership here is approximate and does not take into account all possible biases. For example, small uncertainties in the theoretical colors and magnitudes from the white dwarf models are ignored and there may even be increased intrinsic extinction around these white dwarfs due to the progenitor mass loss.

## 7. DISCUSSION

### 7.1. The Extreme Horizontal Branch of NGC 6791

The CMD of NGC 6791 (Figure 3) clearly shows both a red giant clump and an extremely blue horizontal branch

as discussed earlier. In Figure 7 we take a closer look at these two phases, as well as the white dwarf cooling sequence of the cluster. In the top-right and middle-right panels, we count a total of approximately a dozen stars that are in each of the red giant clump and extreme horizontal branch phases of evolution (over our field area). The presence of both of these core helium burning phases likely suggests that the red giants have undergone stochastic mass loss. In fact, the extremely blue horizontal branch is a likely sign that a fraction of the stars in this cluster have lost an increased amount of mass relative to the “normal” evolution that creates the red giant clump.

An alternate method of producing extreme horizontal branch stars involves binary evolution in which one star loses mass to a companion (see e.g., Han et al. 2003). However, searches for binary companions among globular cluster extreme horizontal branch stars have been unsuccessful (Moni Bidin et al. 2006a,b). Such a scenario is also not likely in NGC 6791. Janes & Kassis (1997) examined the CMDs of about a dozen mostly old open clusters and found that NGC 6791 contains the lowest binary fraction of the group, 14%. The mean fraction among the rest of the sample is 30%. Qualitatively, a large binary fraction for NGC 6791 appears to be ruled out from our much deeper CMD as well. There is no evidence for an obvious equal mass binary sequence nor a very strong signature of extra scatter above the cluster main sequence relative to the CMDs of other rich clusters such as NGC 6819, NGC 2099, NGC 2168, and NGC 2323. All of these other clusters have been shown to contain 20 – 30% binaries through synthetic CMD tests (Kalirai & Tosi 2004). If binary evolution is the cause of the extreme horizontal branch, then it is very unusual that these other clusters do not contain any stars in this phase. In fact, the only other open cluster that shows evidence for an extreme horizontal branch happens to be very similar to NGC 6791 in its fundamental properties. NGC 188 is both an old and metal-rich system and contains two of these hot stars (Dinescu et al. 1996). This strengthens the case for a metallicity-related origin of the extreme horizontal branch stars in these clusters. Binarity also suggests that the extreme horizontal branch stars in NGC 6791 should be centrally concentrated and should contain a significant spread in luminosity, neither of which are observed (Liebert, Saffer, & Green 1994). The derived luminosity range is in fact consistent with that expected from metal-rich, hot horizontal branch stars (Landsman et al. 1998).

Direct photometric and spectroscopic probes to confirm the nature of the extreme horizontal branch stars in NGC 6791 and NGC 188 have largely been unsuccessful. Chaboyer et al. (2002) obtained far ultraviolet images with the Space Telescope Imaging Spectrograph on *HST* to study the possible progenitors of the extreme horizontal branch stars, the bluest of the giant branch stars. If the binary formation theory is correct, then a large fraction of these giants should contain white dwarf companions which could potentially be seen in the ultraviolet. However, in a dozen targeted stars (six in each cluster), none of the NGC 6791 giants and just two of the NGC 188 giants showed a far ultraviolet flux (which may itself come from the chromosphere of the giant star). Detailed abundance analysis of the coolest extreme hori-

zontal branch star in NGC 6791 combined with its optical colors favors it having suffered from heavy line blanketing due to the high metallicity as opposed to a binary nature. Although Green et al. (1997) do find that two of the other NGC 6791 horizontal branch stars are spectroscopic binaries, these two systems are not extremely blue horizontal branch stars.

Taken together, this evidence suggests that the likely cause of the extreme horizontal branch in NGC 6791 is related to the high metallicity of the cluster and not binary evolution. High dispersion observations of the fainter extreme horizontal branch stars (as obtained for the blue horizontal branch stars) could provide the definitive answer.

## 7.2. Avoiding Core Helium Burning

The spectroscopic mass measurement of NGC 6791’s white dwarf population indicates that in addition to a red giant clump and extreme horizontal branch, there is yet a third, even more radical, evolutionary channel for the stars of this cluster. Table 2 indicates that two-thirds of the NGC 6791 *member* white dwarfs have masses below the threshold ( $\sim 0.46 M_{\odot}$ ) at which helium is ignited to produce a carbon-oxygen mixture in the core. This suggests that the progenitor red giants of these stars did not experience a helium flash and therefore bypassed both of the above phases and landed directly on the white dwarf cooling sequence (with helium cores). Such evolution is consistent with models of red giants that suffered extreme mass loss (see section 7.3 – D’Cruz et al. 1996). It is also worth noting that all 12 of the NGC 6791 white dwarfs are DA spectral type. Based on the field white dwarf ratio, we would statistically expect a few of these stars to be DB (helium atmosphere) white dwarfs. A possible explanation for this may be related to the unique evolutionary paths of the progenitor stars which avoided the shell helium burning phase.

The cumulative effect from the post main-sequence evolution of *all* stars in NGC 6791 is shown in the bottom-right panel of Figure 7. The crosses mark all objects on the CMD and the filled (open) circles mark the confirmed (possible field) cluster white dwarfs. Not surprisingly, the bright part of the white dwarf cooling sequence looks unlike that of other star clusters, showing much more scatter. For example, the sequences of the open clusters M67 (Richer et al. 1998) and NGC 6819 (Kalirai et al. 2001b), as well as the globular clusters M4 (Hansen et al. 2004) and NGC 6397 (Richer et al. 2006) exhibit a tighter distribution of points in the faint-blue end of the CMD. Several factors likely contribute to the scatter. First, we noted in §§3 & 6.2 that up to three of the white dwarfs in our sample could potentially be field white dwarfs and therefore there may be a 20 – 30% contamination fraction among all objects (crosses). Second, the masses of the *cluster* white dwarfs, and therefore their core compositions, are different along the cooling sequence. The evolutionary timescales of these stars therefore vary and this would work to wash out a tight cooling sequence. However, if this were the only cause we should see a correlation between the white dwarf masses and their positions in the CMD. Figure 5 shows that this is, in general, not the case. Although it can not be a large effect for the reasons outlined above, some binary evolution may be present in our white dwarf sam-

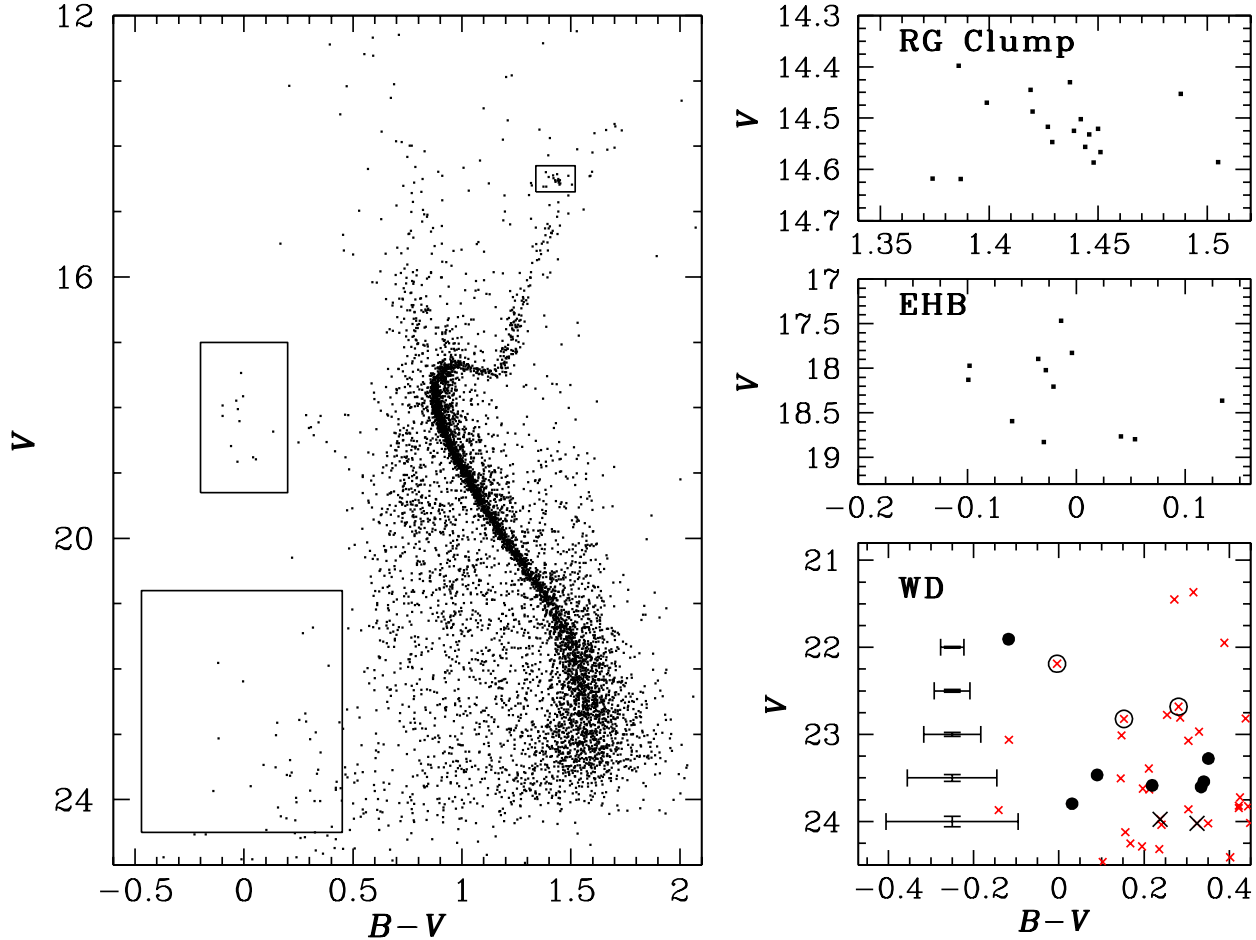


FIG. 7.— A closer look at the red giant clump (RG clump – top-right) and the extreme horizontal branch (EHB – middle-right) of NGC 6791 reveals approximately a dozen stars in each phase. The white dwarf cooling sequence is also shown in the bottom-right panel, along with an indication of the photometric errors in the data. The larger filled (open) circles mark the locations of the confirmed cluster (possible field) white dwarfs in this study. To help illustrate the locations of these three post main-sequence evolutionary phases on the full CMD, we mark boxes on the left-panel corresponding to these zoomed regions.

ple. The spectra of both WD 5 and WD 10 show evidence of contamination, possibly from faint companions. Any mass transfer in the evolution of these systems would certainly alter the subsequent evolution on the white dwarf cooling sequence (see e.g., Hurley & Shara 2003). Although statistically unlikely, it is also possible that we have targeted a double degenerate system. Finally, we have plotted both a  $V$  and  $B - V$  photometric error bar at different magnitudes in the bottom-right panel of Figure 7. The results show that for  $V > 23$  the errors in our colors are comparable to the spread seen in the CMD. This suggests that our photometric errors are also likely dominating the scatter observed on the CMD.

A much better test of the true intrinsic spread along the NGC 6791 white dwarf cooling sequence can be judged from the deep *HST/ACS* CMD of this cluster (Bedin et al. 2005). These data are not affected by photometric errors at these magnitudes. The Bedin et al. (2005) CMD shows clear evidence for a scatter of 0.25 – 0.30 magnitudes (in color) near the tip of the cooling sequence and extending all the way down to the faintest white dwarfs. This rules out photometric errors and therefore the observed spread must be related to the various evolutionary channels that have led to the forma-

tion of these stars, the root of which is the mass loss on the red giant branch. Interestingly, Bedin et al. (2005) find that the location of the reddest white dwarfs along their cooling sequence is consistent with pure helium core models of low mass ( $0.32 M_{\odot}$ ). As we saw in § 6.1, the observed spread in masses of the NGC 6791 white dwarfs ranges from  $0.36 - 0.54 M_{\odot}$  and therefore the dominant bluer sequence of white dwarfs in their CMD (that they fit with carbon-oxygen core models to derive the young age) actually contains a mixture of these canonical white dwarfs (those with progenitors in the red giant clump) and more massive helium core white dwarfs. In our sample of bright white dwarfs, WD 7 ( $M = 0.53 M_{\odot}$ ) likely represents a star that evolved through this normal channel.

### 7.3. Red Giant Branch Mass Loss – Theoretical Estimates

The evolutionary channel discussed above requires some fraction of the stars in NGC 6791 to have experienced enhanced mass loss during their evolution. There are three primary mechanisms for the total post-main sequence mass loss in stars: stationary winds, dust related outflows, and pulsation related outflows (e.g., Willson

2000). The majority of the mass loss takes place while a star is ascending the asymptotic giant branch and evolving through the planetary nebula phase, although the star will also lose an appreciable amount of mass on the red giant branch. It is not well understood whether this latter mass loss, i.e., that occurs prior to the horizontal branch phase, is driven primarily via winds on the red giant branch itself or as a result of the helium flash. However, the amount of the red giant branch mass loss, is a sensitive function of the stellar metallicity, as chemically enriched stars will lose a larger fraction of their total mass.

To estimate the expected mass loss along the red giant branch, we invoke the models of Marigo (2001). These models provide chemical yields for both low- and intermediate- mass stars evolving from the zero age main sequence to the end of the thermally pulsating asymptotic giant branch. The integrated mass loss for a slightly metal-poor ( $[\text{Fe}/\text{H}] = -0.7$ ),  $1.05 M_{\odot}$  star (appropriate mass for an NGC 6791 giant) is 41% of its initial mass. A Solar metallicity star of the same mass will lose 48% of its mass through its evolution. However,  $\sim 40\%$  of the Solar metallicity star's mass loss will occur on the red giant branch whereas 33% of the  $[\text{Fe}/\text{H}] = -0.7$  star's mass loss occurs on the red giant branch. For a metallicity as extreme as NGC 6791's ( $[\text{Fe}/\text{H}] = +0.3 - +0.5$ ), a star will lose even a larger fraction of its mass on the red giant branch. D'Cruz et al. (1996) estimate that a  $1.08 M_{\odot}$  star with  $[\text{Fe}/\text{H}] = +0.37$  will form a core with a mass of just  $0.45 - 0.47 M_{\odot}$ .

These theoretical calculations suggest that the amount of mass loss along the red giant branch of NGC 6791 will yield a final mass of the star at the tip of the branch that is within a few-hundredths of the critical mass needed to ignite helium in the core. Given the stochastic nature of the red giant branch mass loss, some stars in NGC 6791 certainly reached the critical mass whereas others did not. The large internal metallicity dispersion within the cluster ( $\text{rms} = 0.08 \text{ dex}$  – Gratton et al. 2006) will also add to the variable mass loss. For example, Worthey & Jowett (2003) present low-resolution spectra of K giants and find that one star in this cluster has an extremely high metal abundance,  $[\text{Fe}/\text{H}] = +0.6$ . The theoretical arguments for this mass loss are therefore qualitatively consistent with our conclusions above based on the morphology of the NGC 6791 CMD and the masses of the cluster white dwarfs.

#### 7.4. The Luminosity Function of NGC 6791's Red Giant Branch

If, in fact, a significant fraction of NGC 6791's stellar population is peeling away from the red giant branch before the helium flash, then the luminosity function of the cluster's red giant branch should be depleted as one approaches the tip (see e.g., Sandquist & Martel 2007). An analysis of the cluster's red giant branch by Garnavich et al. (1994) found that its tip does not rise above  $M_I \sim -2.7$ , over a magnitude fainter than metal-rich globular clusters. Interestingly, the recent study of Luck & Heiter (2007) compares the metallicity distribution functions of nearby field dwarfs and giants, and finds that the giant distribution lacks a metal-rich tail. To test whether there is a *thinning* out of this upper red giant branch, we compare the cluster's red giant branch luminosity function

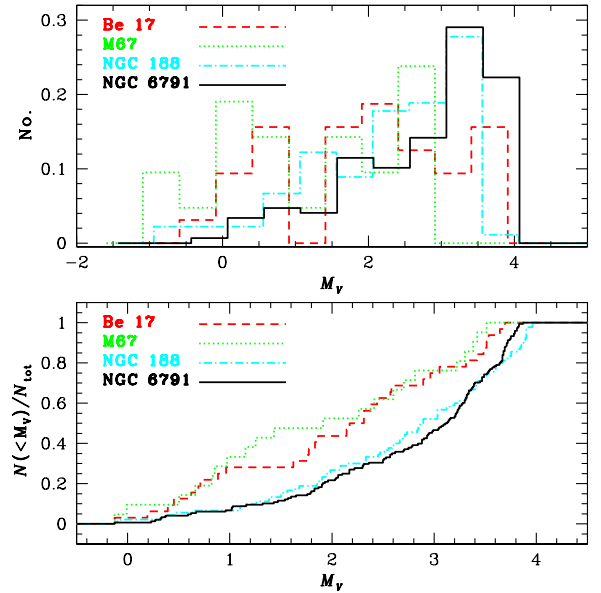


FIG. 8.— The differential (top) and cumulative (bottom) red giant branch luminosity function of NGC 6397 (solid) is compared to those of three other old open clusters, Berkeley 17 (dashed), M67 (dotted), and NGC 188 (short dash-dot). Both panels indicate that the number of red giants in NGC 6791 decreases more rapidly than the other clusters as the tip is approached. As discussed in the text, this *thinning* out of the upper red giant branch suggests that stars are peeling away, never having experienced a helium flash, and forming undermassive helium core white dwarfs.

to that of three other old open star clusters, Berkeley 17 (8.5 Gyr – Bragaglia et al. 2006), M67 (4.3 Gyr – Richer et al. 1998), and NGC 188 (6.8 Gyr – Stetson, McClure, & Vandenberg 2004 and references within). We isolate the red giant branch stars from the published CMDs in these studies and apply the derived distance moduli to each data set. We also confirmed that our study is not incomplete near the tip of the red giant branch, where these stars become increasingly redder. For this, we matched our optical data to the near infrared study of Carney, Lee, & Dodson (2005) and were able to recover all of the red giants near the tip.

Figure 8 (top) shows the red giant branch luminosity function for each cluster. We have plotted this with the tip of the branch towards the left of the diagram. Both in NGC 188 (also a metal-rich cluster) and NGC 6791, the luminosity functions are heavily skewed towards the base of the red giant branch. The decline in the number of stars as the tip is approached is more rapid in NGC 6791 than in all three other clusters. To illustrate this more clearly, we build cumulative luminosity functions for each cluster in Figure 8 (bottom) and adjust each function so the brightest observed giant is shifted to a common magnitude. This aligning of the tip of the red giant branch has the advantage that it is largely independent of both chemical composition and age (Sandquist & Martel 2007). The NGC 6791 luminosity function is clearly “bottom-heavy” relative to the other clusters, suggesting that there is an absence of red giants near the tip. This absence is not caused by very red stars that may have escaped detection in our study. To test this further, we apply a Kolmogorov-Smirnov (K-S) test (Press, Flannery, & Teukolsky 1986) between the NGC 6791 luminosity function and each of the other three clusters.

The K-S test makes no assumption about the distribution of the data and is therefore insensitive to possible spurious biases from arbitrary binning of data. The significance level probability,  $P$ , that the null hypothesis is true (i.e., that the luminosity functions are drawn from the same distribution) is found to be  $<0.01$  when comparing NGC 6791 to each of Berkeley 17 and M67. For the two more metal-rich clusters with extreme horizontal branches, NGC 6791 and NGC 188, the K-S test yields a probability  $P = 0.31$  (i.e., it can not be shown that these two luminosity functions are drawn from different distributions).

### 7.5. Resolving the Age Discrepancy of NGC 6791

The observed white dwarfs in our sample are the brightest objects along the cooling sequence whereas most of the leverage in measuring the white dwarf cooling age of the cluster comes from fainter white dwarfs in the Bedin et al. (2005) peak. Over these magnitudes, stars along this cooling sequence have a very small change in mass (also true for their progenitors). Therefore, the same fate should affect all of these stars unless we have not accounted for a piece of missing physics. Hansen (2005) estimated the number of white dwarfs in the Bedin et al. CMD that came from each of the three evolutionary channels by considering the lifetimes of stars in the red giant clump, extreme horizontal branch, and white dwarf cooling phases, and by assuming a ratio of extreme horizontal branch stars to red giant clump stars in those data. The CMD presented in Figure 7 overlaps the *HST*/ACS study and so we can now refine this calculation. Over the ACS field targeted by Bedin et al., the CMD of NGC 6791 shows two extreme horizontal branch stars and four red giant clump stars. The evolutionary timescale for these core helium burning phases lasts approximately  $1 \times 10^8$  years, whereas the cooling time for the faintest white dwarfs in the HST study is  $\sim 2 \times 10^9$  years (for carbon-oxygen core models down to  $F606W = 28$ ). Therefore, scaling arguments suggest that 120 of the white dwarfs in the Bedin et al. study should have evolved from either of these two evolutionary channels and therefore have carbon-oxygen cores (two-thirds of which came from the canonical red giant clump phase). The white dwarf cooling sequence of the cluster shows roughly 600 white dwarfs, and therefore up to 80% of the white dwarfs may be helium core stars.

An independent check on these numbers can now be derived from our mass measurements. Figure 9 indicates that the ratio of helium-core to carbon-oxygen core white dwarfs in NGC 6791 is  $\sim 2:1$ , assuming that  $0.46 M_{\odot}$  is the threshold at which a carbon-oxygen core will be produced in the progenitor star. If this critical mass is slightly larger, i.e.,  $0.48 M_{\odot}$ , then the ratio may be as large as 8:1. Since the cooling is a factor of  $\sim 3 \times$  slower for the helium core stars, their cluster birthrate is then estimated to be between 40 – 70% of all stars.

The fraction of helium core vs carbon-oxygen core white dwarfs directly affects the inferred cluster white dwarf cooling age as the cooling rates are proportional to the mass number (chemical species) of the core. For example, for a fixed stellar mass, a 50/50 carbon-oxygen mixture will have  $\sim 3.5 \times$  fewer ions than a helium core star. This results in a higher heat capacity for the helium core white dwarf and therefore the cooling will be

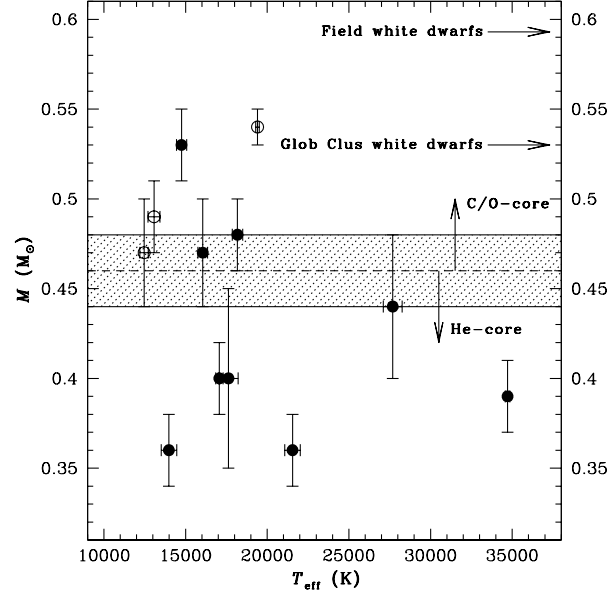


FIG. 9.— The  $M$ – $T_{\text{eff}}$  plane for all confirmed NGC 6791 white dwarfs (solid points) as well as those that were determined to be  $2\sigma$  outliers from cluster membership in § 6.2 (open circles). Six of the nine cluster white dwarfs clearly have a mass under the threshold (hashed region –  $M \sim 0.46 M_{\odot}$ ) at which helium would have been ignited in the core of the progenitor star to produce carbon-oxygen. The arrow marks the mean mass of the field white dwarf distribution from the Sloan Digital Sky Survey ( $0.59 M_{\odot}$ ) and the mean mass of the globular cluster NGC 6752's white dwarf population ( $0.53 M_{\odot}$  – Moehler et al. 2004). All of our cluster white dwarfs have a mass less than these values.

$\sim 3.5 \times$  slower than that of a carbon-oxygen core white dwarf of similar mass. This is of course offset slightly by the fact that the mean mass of the helium core stars is somewhat smaller than that of normal carbon-oxygen core white dwarfs (a relatively small effect in this case). By comparing the observed white dwarf luminosity function to model luminosity functions that invoke pure helium cores, pure carbon-oxygen cores, and a combination of the two, Hansen (2005) was able to show that an age of 7–8 Gyr requires the birthrate fraction of helium core white dwarfs in the cluster to be between 50% and 100% of the total white dwarf production. This is consistent with our findings above.

### 7.6. The Ultraviolet Upturn in Elliptical Galaxies

The ultraviolet upturn in elliptical galaxies and spiral bulges refers to the sharp, rising flux in the integrated spectra of these objects shortward of  $\lambda \sim 2500$  Å (Burstein et al. 1988; Gregg & Renzini 1990; Bressan, Chiosi, & Fagotto 1994; O'Connell 1999; Brown 2004). The phenomenon is found to be extremely variable in different galaxies, and therefore must be very sensitive to the properties of the sources responsible for the upturn. The dominant, old main-sequence stellar population of these galaxies is too faint, and cool, to constitute any appreciable fraction of this flux. Therefore, the sources must either be young massive stars (e.g., in active star formation regions) or more exotic populations of low-mass, hot stars. Recent results from GALEX suggest that only in rare cases does the former dominate the ultraviolet flux (Salim et al. 2005; Rich et al. 2005; Donas et al. 2006). For the latter, Gregg & Renzini (1990) consider the energetics of several possible sources includ-

ing binary candidates, hot or accreting white dwarfs, post asymptotic giant branch stars, and extreme horizontal branch stars and find that the extreme horizontal branch stars are the most likely candidates (although, see recent study by Han, Podsiadlowski, & Lynas-Gray 2007 suggesting a binary model for the excess). These stars are hot, bright, and can establish an equilibrium while burning helium in their cores for  $\sim 10^8$  years. Unfortunately, resolved photometry, or spectroscopy, of the sources for the ultraviolet upturn in these distant galaxies is currently not possible (although M31 and M32 have been imaged in the ultraviolet - Bertola et al. 1995; Brown et al. 2000).

In Galactic globular clusters extremely blue horizontal branches have long been argued to exist because of the system's old age, low metallicity, and differential mass loss on the red giant branch (Iben & Rood 1970). However, the properties of these systems (e.g., low metallicity, high density) are contrary to the extragalactic populations (Liebert, Saffer, & Green 1994). Recent studies have shown that metal-rich disk clusters also possess an extended blue horizontal branch (e.g., Rich et al. 1997), thereby providing nearby systems, with some similar properties to the elliptical galaxies and spiral bulges, that possibly harbor the sources causing the ultraviolet upturn. Given its old age, very high metal abundance, and small distance modulus, NGC 6791 represents a nearby analog of the metal-rich component in these galaxies that can be used to understand the origin of the extra far-ultraviolet radiation (see also Liebert, Saffer, & Green 1994).

We have shown that the white dwarf population of NGC 6791 is undermassive, a consequence of enhanced mass loss in the evolution of the progenitors of these stars. The extreme horizontal branch stars of NGC 6791 are a subset of this population, those that lost mass on the red giant branch but not enough to prevent the ignition of helium while the star was well on its way to becoming a white dwarf. This type of evolution clearly suggests that even within a co-eval system with little metallicity spread, the mass loss is variable. Of course this effect would be compounded in a system such as an elliptical galaxy which has a large spread in both metallicity and age relative to an open cluster. Furthermore, as we mentioned earlier, the amount of ultraviolet flux in these galaxies is found to vary enormously from galaxy to galaxy. The variable excess likely depends sensitively on the number of extreme horizontal branch stars and could even be susceptible to their specific location along the extreme horizontal branch. The stochastic mass loss, due to the metallicity, could therefore be a contributor in dictating the amount of this ultraviolet flux in ellipticals and spiral bulges. Other sources, such as the presence of a minority population of helium enhanced stars (Piotto et al. 2005), may also be important.

In total, about 30% of the NGC 6791 helium burning stars are hot (including the new ones found by Buson et al. 2006). Of course, this is an extreme case considering the very high metallicity of the cluster; slightly lower metallicity populations are expected to produce a smaller fraction. Dorman, O'Connell, & Rood (1995) construct synthetic population models and find that even for the bluest galaxies, a fraction of just 15 – 20% of the stars would need to become extreme horizontal branch stars

to explain the ultraviolet colors. Therefore the production of extreme horizontal branch stars in an environment such as NGC 6791 is certainly sufficient to explain the ultraviolet upturn in elliptical galaxies and spiral bulges. If, in fact, the amount of excess ultraviolet radiation in these systems increases with metallicity, then this could directly correlate with the picture of enhanced mass loss in metal-rich systems that would produce a larger fraction of the sources of the radiation. However, the jury is still out on whether such a trend exists. For example, Burstein et al. (1988) see a positive correlation between the ultraviolet excess and metallicity whereas other studies do not (e.g., Rich et al. 2005).

## 8. CONCLUSIONS

We have presented the first spectroscopic observations of the white dwarf population of the metal-rich open star cluster NGC 6791. Two-thirds of the white dwarfs in this cluster are found to be undermassive, well below the  $M \sim 0.46 M_{\odot}$  threshold at which helium would have ignited in the cores of the progenitor red giant branch stars to produce carbon-oxygen. These helium-core white dwarfs have formed in this cluster as a result of enhanced mass loss on the red giant branch, due to the high metallicity of the cluster ( $[\text{Fe}/\text{H}] \sim +0.4$ ). This scenario naturally provides an explanation for the recently reported low white dwarf cooling age of NGC 6791 by Bedin et al. (2005); helium-core white dwarfs cool a factor of  $\sim 3 \times$  slower than carbon-oxygen core white dwarfs and therefore their measurement of 2.4 Gyr would actually imply a cooling age of  $\gtrsim 7$  Gyr, consistent with the well measured main-sequence turnoff age. The enhanced mass loss also explains the presence of the extreme horizontal branch stars in this cluster which are plausible analogs of the sources responsible for the ultraviolet upturn in elliptical galaxies and spiral bulges.

Interestingly, a recent study by Kilic, Stanek, & Pinsonneault (2007) has reported that there is a significant analogous field population of low mass, single white dwarfs that arises from old, metal-rich stars that suffered severe mass loss and avoided the helium flash. Therefore, the results in this paper are likely a general consequence of stellar evolution in high metallicity environments.

Finally, it is worth noting that these results do not rule out that the cooling rate of some of NGC 6791's white dwarfs has been retarded from the sedimentation of  $^{22}\text{Ne}$  (Deloye & Bildsten 2002).  $^{22}\text{Ne}$  is produced during helium burning and so the helium core white dwarfs would be unaffected, however, this could represent a heating mechanism for the carbon-oxygen core stars. The rate at which  $^{22}\text{Ne}$  settles into the core depends on internal physics that are currently not well understood. Further investigation of this heating source will likely clarify how dominant this effect is in a metal-rich environment such as NGC 6791. Other explanations related to white dwarf physics, binarity, or enhanced helium abundances may yet emerge. Future observations of NGC 6791 may be able to confirm our picture. Ground based observations of the cluster red giants in the mid-infrared could potentially show signs of the enhanced mass loss (e.g., through a 10 micron excess). A deeper study of the cluster white dwarfs should also be undertaken with *HST*. Such observations should unveil a second peak in the white dwarf luminosity function resulting from the cooling of canoni-

cal carbon-oxygen core white dwarfs. The second epoch data could also provide for a much cleaner study of cluster stars through proper motion selection.

We gratefully acknowledge L. Bildsten for reading our manuscript before submission and suggesting several useful additions and clarifications related to the cooling of white dwarfs. We wish to also acknowledge help from D. Leong and E. Chudwick with data processing. We are grateful to R. Peterson and B. Holden for insightful discussions related to extreme horizontal branch stars and the ultraviolet upturn in elliptical galaxies. We thank S. Kepler for kindly providing us with the list of

magnitudes and masses for the sample of white dwarfs in the Sloan Digital Sky Survey. JSK is supported by NASA through Hubble Fellowship grant HF-01185.01-A, awarded by the Space Telescope Science Institute, which is operated by the Association of Universities for Research in Astronomy, Incorporated, under NASA contract NAS5-26555. Support for this work was also provided by grant HST-GO-10424 from NASA/STScI. PB is a Cottrell Scholar of Research Corporation. The research of PB and HBR is supported by grants from the Natural Sciences and Engineering Research Council of Canada. HBR also thanks the Canada-US Fulbright Program for the award of a Fulbright Fellowship.

## REFERENCES

Allard, F., Wesemael, F., Fontaine, G., Bergeron, P., & Lamontagne, R. 1994, AJ, 107, 1565

Bedin, L. R., Salaris, M., Piotto, G., King, I. R., Anderson, J., Cassisi, S., & Momany, Y. 2005, ApJ, 624, L45

Bergeron, P., Saffer, R. A., & Liebert, J. 1992, ApJ, 394, 228

Bergeron, P., Liebert, J., & Fulbright, M. S. 1995, AJ, 444, 810

Bertola, F., Bressan, A., Burstein, D., Buson, L. M., Chiosi, C., & di Serego Alighieri, S. 1995, ApJ, 438, 680

Bragaglia, A., Tosi, M., Andreuzzi, G., & Marconi, G. 2006, MNRAS, 368, 1971

Bressan, A., Chiosi, C., & Fagotto, F. 1994, ApJS, 94 63

Brown, T. M., Bowers, C. W., Kimble, R. A., Sweigart, A. V., & Ferguson, H. C. 2004, ApJ, 532, 308

Brown, T. M. 2004, ApSS, 291, 215

Burstein, D., Bertola, F., Buson, L. M., Faber, S. M., & Lauer, T. R. 1988, ApJ, 328, 440

Buson, L. M., Bertone, E., Buzzoni, A., & Carraro, G. 2006, Baltic Astronomy, 15, 49

Carney, B. W., Lee, J.-W., & Dodson, B. 2005, AJ, 129, 656

Carraro, G., Villanova, S., Demarque, P., McSwain, M. V., Piotto, G., & Bedin, L. R. 2006, ApJ, 643, 1151

Castellani, M., & Castellani, V. 1993, ApJ, 407, 649

Chaboyer, B., Green, E. M., & Liebert, J. 1999, AJ, 117, 1360

Chaboyer, B., Dambach, E., Green, E. M., & Landsman, W. B. 2002, Bulletin of the American Astronomical Society, 34, 1128

Claver, C. F., Liebert, J., Bergeron, P., & Koester, D. 2001, ApJ, 563, 987

D'Cruz, N. L., Dorman, B., Rood, R. T., & O'Connell, R. W. 1996, ApJ, 466, 359

Deloye, C. J., & Bildsten, L. 2002, ApJ, 580, 1077

Demarque, P., Green, E. M., & Guenther, D. B. 1992, AJ, 103, 151

Dinescu, D. I., Girard, T. M., van Altena, W. F., Yang, T.-G., & Lee, Y.-W. 1996, AJ, 111, 1205

Dominguez, I., Chieffi, A., Limongi, M., & Straniero, O. 1999, ApJ, 524, 226

Donas, J., et al. 2006, ApJS, in press (astro-ph/0608594)

Dorman, B., O'Connell, R. W., & Rood, R. T. 1995, ApJ, 442, 105

Faulkner, J. 1972, ApJ, 172, 401

Fontaine, G., Brassard, P., & Bergeron, P. 2001, PASP, 113, 409

Friel, E. D., & Janes, K. A. 1993, A&A, 267, 75

Garnavich, P. M., Vandenberg, D. A., Zurek, D. R., & Hesser, J. E. 1994, AJ, 107, 1097

Gratton, R., Bragaglia, A., Carretta, E., & Tosi, M. 2006, ApJ, 642, 462

Green, E. M., Liebert, J., & Peterson, R. C. 1996, in ASP Conf. Ser. 92: Formation of the Galactic Halo...Inside and Out, 184

Green, E. M., Liebert, J. W., Peterson, R., & Saffer, R. A. 1997, The Third Conference on Faint Blue Stars, Edited by A. G. D. Philip, J. Liebert, R. Saffer and D. S. Hayes, Published by L. Davis Press, 271

Greggio, L., & Renzini, A. 1990, ApJ, 364, 35

Han, Z., Podsiadlowski, Ph., Maxted, P. F. L., & Marsh, T. R. 2003, MNRAS, 341, 669

Han, Z., Podsiadlowski, Ph., & Lynas-Gray, A. E. 2007, MNRAS, 380, 1098

Hansen, B. M. S., & Phinney, E. S. 1998, MNRAS, 294, 557

Hansen, B. M. S., Richer, H. B., Fahlman, G. G., Stetson, P. B., Brewer, J., Currie, T., Gibson, B. K., Ibata, R., Rich, R. M., & Shara, M. M. 2004, ApJS, 155, 551

Hansen, B. M. S. 2005, ApJ, 635, 522

Hansen, B. M. S. et al. 2007, ApJ, in press, astro-ph/0701738

Hurley, J. R., & Shara, M. M. 2003, ApJ, 589, 179

Iben, Jr., I., & Rood, R. T. 1970, ApJ, 161, 587

Janes, K., & Kassis, M. 1997, in ASP Conf Ser. 130: The Third Pacific Rim Conference on Recent Development on Binary Star Research, 107

Kalirai, J. S., Richer, H. B., Fahlman, G. G., Cuillandre, J., Ventura, P., D'Antona, F., Bertin, E., Marconi, G., & Durrell, P. 2001a, AJ, 122, 257

Kalirai, J. S., Richer, H. B., Fahlman, G. G., Cuillandre, J., Ventura, P., D'Antona, F., Bertin, E., Marconi, G., & Durrell, P. 2001b, AJ, 122, 266

Kalirai, J. S., Ventura, P., Richer, H. B., Fahlman, G. G., D'Antona, F., & Marconi, G. 2001c, AJ, 122, 3239

Kalirai, J. S., Fahlman, G. G., Richer, H. B., & Ventura, P. 2003, AJ, 126, 1402

Kalirai, J. S. & Tosi, M. 2004, MNRAS, 351, 649

Kalirai, J. S., Richer, H. B., Reitzel, D., Hansen, B. M. S., Rich, R. M., Fahlman, G. G., Gibson, B. K., & von Hippel, T. 2005a, ApJ, 618, L123

Kaluzny, J. 1990, MNRAS, 243, 492

Kaluzny, J., & Udalski, A. 1992, Acta Astronomica, 42, 29

Kaluzny, J., & Rucinski, S. M. 1995, A&AS, 114, 1

Kelson, D. D., Illingworth, G. D., van Dokkum, P. G., & Franx, M. 2000, ApJ, 531, 159

Kelson, D. 2003, PASP, 115, 688

Kepler, S. O., Kleinman, S. J., Nitta, A., Koester, D., Castanheira, B. G., Giovannini, O., Costa, A. F. M., & Althaus, L. 2007, MNRAS, 375, 1315

Kilic, M., Stanek, K. Z., & Pinsonneault, M. H. 2007, ApJ, submitted, astro-ph/0706.3045

King, I. R., Bedin, L. R., Piotto, G., Cassisi, S., & Anderson, J. 2005, AJ, 130, 626

Kinman, T. D. 1965, ApJ, 142, 655

Landsman, W., Bohlin, R. C., Neff, S. G., O'Connell, R. W., Roberts, M. S., Smith, A. M., & Stecher, T. P. 1998, AJ, 116, 789

Lanz, T., Brown, T. M., Sweigart, A. V., Hubeny, I., & Landsman, W. B. 2004, ApJ, 602, 342

Liebert, J., Bergeron, P., & Holberg, J. B. 2005, ApJS, 156, 47

Liebert, J., Saffer, R. A., & Green, E. M. 1994, AJ, 107, 1408

Luck, R. E., & Heiter, U. 2007, AJ, 133, 2464

Marigo, P. 2001, A&A, 370, 194

Mathieu, R. D. 2000, in ASP Conf. Ser. 198: Stellar Clusters and Associations: Convection, Rotation, and Dynamics, 517

Maxted, P. f. L., Heber, U., Marsh, T. R., & North, R. C. 2001, MNRAS, 326, 1391

Moehler, S., Koester, D., Zoccali, M., Ferraro, F. R., Heber, U., Napiwotzki, R., & Renzini, A. 2004, A&A, 420, 515

Moni Bidin, C., Moehler, S., Piotto, G., Recio-Blanco, A., Momany, Y., & Mendez, R. A. 2006a, A&A, 451, 499

Moni Bidin, C., Moehler, S., Piotto, G., Momany, Y., Recio-Blanco, A., & Mendez, R. A. 2006b, "Globular Clusters: Guides to Galaxies", astro-ph/0606035

Montgomery, K. A., Janes, K. A., & Phelps, R. L. 1994, AJ, 108, 585

O'Connell, R. W. 1999, ARA&A, 37, 603

Oke, J. B. 1995, PASP, 107, 375

Origlia, L., Valenti, E., Rich, R. M., & Ferraro, F. R. 2006, *ApJ*, 646, 499

Perryman, M. A. C., Brown, A. G. A., Lebreton, Y., Gomez, A., Turon, C., de Strobel, G. C., Mermilliod, J. C., Robichon, N., Kovalevsky, J., & Crifo, F. 1998, *A&A*, 331, 81

Peterson, R. C., & Green, E. M. 1998, *ApJ*, 502, L39

Pietrinferni, A., Cassisi, S., Salaris, M., & Castelli, F. 2004, *ApJ*, 612, 168

Piotto, G. et al. 2005, *ApJ*, 621, 777

Press, W. H., Flannery, B. P., & Teukolsky, S. A. 1986, *Numerical Recipes*, Cambridge: Cambridge Univ. Press

Rich, R. M., et al. 1997, *ApJ*, 484, L25

Rich, R. M., et al. 2005, *ApJ*, 619, L107

Richer, H. B., Fahlman, G. G., Rosvick, J., & Ibata, R. 1998, *ApJ*, 504, L91

Richer, H. B. et al. 2006, *Science*, 313, 936

Salaris, M., Garcia-Berro, E., Hernanz, M., Isern, J., & Saumon, D. 2000, *ApJ*, 544, 1036

Salim, S., et al. 2005, *ApJ*, 619, L39

Sandquist, E. L., & Martel, A. R. 2007, *ApJ*, 654, L65

Spinrad, H., & Taylor, B. J. 1971, *ApJ*, 163, 303

Stetson, P. B. 1994, *PASP*, 106, 250

Stetson, P. B., Brunett, H., & Grundahl, F. 2003, *PASP*, 115, 413

Stetson, P. B., McClure, R. D., & VandenBerg, D. A. 2004, *PASP*, 116, 1012

Sweigart, A. V. 1987, *ApJS*, 65, 95

VandenBerg, D. A., Bergbusch, P. A., & Dowler, P. D. 2005, *ApJS*, 162, 375

von Hippel, T., Steinhauer, A., Sarajedini, A., & Deliyannis, C. P. 2002, *AJ*, 124, 1555

von Hippel, T. 2005, *ApJ*, 622, 565

Willson, L. A. 2000, *ARA&A*, 38, 573

Worthey, G., & Jowett, K. J. 2003, *PASP*, 115, 96

Yong, H., Demarque, P., & Yi, S. 2000, *ApJ*, 539, 928